Dissecting the DNA binding landscape and gene regulatory network of p63 and p53

Konstantin Riege[1], Helene Kretzmer[2], Arne Sahm[1], Simon S. McDade[3], Steve Hoffmann[1], Martin Fischer[1,#]

[1] Computational Biology Group, Leibniz Institute on Aging – Fritz Lipmann Institute (FLI), Beutenbergstraße 11, 07745 Jena, Germany

[2] Department of Genome Regulation, Max Planck Institute for Molecular Genetics, Ihnestraße 63-73, 14195 Berlin, Germany

[3] Patrick G Johnston Centre for Cancer Research, Queen's University Belfast, 97 Lisburn Road, Belfast BT9 7AE, UK

Running title: p63 GRN vs p53 GRN

[#]To whom correspondence should be addressed. Email: Martin.Fischer@leibniz-fli.de

Abstract

The transcription factor (TF) p53 is the best-known tumor suppressor, but its ancient sibling p63 (ΔNp63) is a master regulator of epidermis development and a key oncogenic driver in squamous cell carcinomas (SCC). Despite multiple gene expression studies becoming available in recent years, the limited overlap of reported p63-dependent genes has made it difficult to decipher the p63 gene regulatory network (GRN). In particular, analyses of p63 response elements differed substantially among the studies. To address this intricate data situation, we provide an integrated resource that enables assessing the p63-dependent regulation of any human gene of interest. Here, we use a novel iterative *de novo* motif search approach in conjunction with extensive publicly available ChIP-seq data to achieve a precise global distinction between p53 and p63 binding sites, recognition motifs, and potential co-factors. We integrate all these data with enhancer:gene associations to predict p63 target genes and identify those that are commonly de-regulated in SCC and, thus, may represent candidates for therapeutic interventions.

Keywords

p63, p53, gene regulation, DNA binding, squamous cell carcinoma

Introduction

In contrast to the tumor suppressor p53 with its extensive set of target genes controlling the cell cycle and apoptosis (Fischer, 2017; Sammons et al., 2020), its phylogenetically ancient sibling p63 governs epidermis development (Mills et al., 1999; Yang et al., 1999) and is an oncogenic driver of squamous cell carcinoma (SCC) (Campbell et al., 2018; Gatti et al., 2019) that is overexpressed or amplified in SCCs, which depend on its expression (Ramsey et al., 2013). Together with p73, p63 and p53 form the p53 transcription factor (TF) family that shares a highly conserved DNA binding domain (DBD) through which they bind to very similar DNA recognition motifs. The mechanisms that enable these sibling TFs to shape their unique gene regulatory network (GRN) leading to the different phenotypic control, however, remain poorly understood.

The *TP53* and *TP63* genes encode for two major isoform groups that are controlled by distinct promoters leading to transcripts differing in their N-terminus (Murray-Zmijewski et al., 2006). In the case of *TP53*, the longest isoform, p53α, is ubiquitously expressed while the alternative intronic promoter has little activity across virtually all tissues. Conversely, the usage of the two *TP63* promoters is highly cell type-dependent. For instance, the long isoform TAp63 is predominantly expressed in germ cells, while the smaller transcript, ΔNp63, is most copious in stratifying epithelia (Sethi et al., 2015). Similar to p53, alternative splicing leads to α, β, and γ protein isoforms that differ in their C-terminus (Murray-Zmijewski et al., 2006). While both TAp63 and ΔNp63 may bind to DNA through a specific binding domain, ΔNp63 lacks the canonical N-terminal transactivation domain (TAD) (Yang et al., 1998) and has long been thought to be a dominant-negative regulator of other p53 family members or its own isoforms (Gebel et al., 2016; Yang et al., 1998). However, ΔNp63 has also been shown to harbor alternative TADs, that endow transactivation activity (Helton et al., 2006; King et al., 2003; Yang et al., 2006). Notably, the many ΔNp63 binding sites are associated with enhancer regions, where ΔNp63 has been proposed to “bookmark” genes that are expressed in stratifying epithelia (Karsli Uzunbas et al., 2019; Kouwenhoven et al., 2015a; Lin-Shiao et al., 2019; Qu et al., 2018; Somerville et al., 2018). Here, we focus on the most widely expressed isoforms p53α (hereafter p53) and ΔNp63 (hereafter p63).

The p53 TF family shares many binding sites, but all three family members have been shown to bind to substantial sets of unique target genes (Lin et al., 2009; McDade et al., 2014). Indeed, there are differences in the DBDs, e.g. regarding thermostability, hydrophobic potentials (Enthart et al., 2016), zinc-coordination (Lokshin et al., 2007), and redox sensitivity (Tichý et al., 2013). In addition, the different C-terminal domains (CTD) of p53 family members may also affect their DNA binding specificity (Sauer et al., 2008). p53 binds to a canonical 20 bp response element (RE) made of two decameric half-sites that both contain the sequence

RRRCWWGYYY (R = A/G; W= A/T; Y = C/T). p53 has also been shown to bind to decameric half-sites separated by spacers or to single half-sites (Kitayner et al., 2010; Menendez et al., 2013; Vyas et al., 2017). Results from systematic evolution of ligands by exponential enrichment (SELEX) (Ortt and Sinha, 2006; Perez et al., 2007) and high-throughput analyses of chromatin immunoprecipitation (ChIP) (Kouwenhoven et al., 2010; McDade et al., 2012; Yang et al., 2006) yielded p63 binding motifs with high similarity to the p53RE but still showed some unique characteristics. These unique characteristics identified for p63REs, however, differed substantially between the studies.

While multiple genome-wide p63 gene expression datasets became available in recent years, our understanding of the p63 GRN remains incomplete. This is in part due to the limited overlap of the p63-dependent genes identified in individual studies (Kouwenhoven et al., 2015b). Also, the frequent binding of p63 to enhancers (Kouwenhoven et al., 2015a; Lin-Shiao et al., 2018, 2019; Qu et al., 2018; Somerville et al., 2018) and the difficulty to associate such enhancers with target gene regulation adds another level of complexity to the quest of describing the GRN. To overcome these limitations, we utilize a recently developed meta-analysis approach (Fischer et al., 2016a), which helped us to dissect the GRNs of the mouse and human orthologue of p53 (Fischer, 2019). The analysis rests upon a ranking of potential p63 target genes based on the number of datasets supporting a p63-dependent regulation. In addition, we utilize the wealth of recent p63 and p53 ChIP-seq studies to establish a more precise global distinction between p53 and p63 binding sites and their underlying REs. This approach could serve as a blueprint to distinguish binding site specificities of TF siblings. Further integration of gene expression studies with the binding data and enhancer:gene associations enables us to predict high-probability direct p63 target genes.

Results

The p63 gene regulatory network

To identify genes commonly regulated by p63 across cell types and tissues, we employed a previously established meta-analysis approach, that has been helpful to infer core GRNs for human and mouse p53, the viral oncoprotein E7 and the cell cycle GRN (Fischer, 2019; Fischer et al., 2014, 2016a, 2017). From 11 genome-wide studies (Abraham et al., 2018; Bao et al., 2015; Carroll et al., 2006; Gallant-Behm et al., 2012; Karsli Uzunbas et al., 2019; Lin-Shiao et al., 2019; Saladi et al., 2017; Somerville et al., 2018; Watanabe et al., 2014; Wu et al., 2012; Zarnegar et al., 2012) (Supplementary Table 1), 16 publically available gene expression datasets were integrated to generate a specific *p63 Expression Score* (Supplementary Table 2). The datasets have been obtained from knockdown (n=12) or overexpression experiments (n=4) of p63 in primary keratinocytes (n=3), the keratinocyte cell

line HaCaT (n=2), the foreskin fibroblast cell line BJ (n=1), the breast epithelial cell line MCF10A (n=4), the squamous carcinoma cell lines H226 (n=2), KYSE70 (n=1), and FaDu (n=1), as well as the pancreatic ductal adenocarcinoma cell lines BxPC3 (n=1) and SUIT2 (n=1) (Figure 1A and 1B).

To illustrate the utility of our approach, we selected 30 genes from various *p63 Expression Score* groups reflecting commonly up- and down-regulated ones (Figure 1C). We noted lower consistency across the data on p63-dependent gene regulation as compared to previous meta-analyses on human and mouse p53 (Fischer, 2019; Fischer et al., 2016a). In contrast to the recent investigations, data integrated here are based on a higher number of experiments in primary cells and a comparably lower number of replicates. Thus, the reduced consistency may also reflect the higher variance as opposed to data from more homogenous cell lines. Furthermore, p63-depleted cells are less viable, and the global decrease in mRNA levels may confound effects. Despite this, our approach identified genes that are commonly altered by p63.

We next performed gene set enrichment analysis (GSEA) for p63-dependently regulated genes using MSigDB gene sets (Subramanian et al., 2005). In agreement with the function of p63 as an essential proliferation factor (McDade et al., 2011; Senoo et al., 2007; Truong et al., 2006), epidermal development regulator (Mills et al., 1999; Yang et al., 1999), and MYC network activator (Wu et al., 2012), we find that genes commonly up-regulated by p63 significantly enrich gene sets associated with cell cycle, epidermis development, and MYC targets (Figure 2A). In line with previous reports (Mehta et al., 2018), genes down-regulated by p63 enrich gene sets connected with interferon response (Figure 2B). Corroborating the role of p63 in mammary stem cell activity (Chakrabarti et al., 2014) and SCC growth (Ramsey et al., 2013), we find that p63 up- and down-regulated genes enrich respective gene sets up- and down-regulated in mammary stem cells (Figure 2C) and across SCCs (Figure 2D). In addition to pathways that have been linked to p63 earlier, we find that p63 up-regulated genes enrich for mTORC1 signaling genes and p63 down-regulated genes enrich for gene sets associated with oxidative phosphorylation and aerobic respiration (Figure 2E).

Further, we performed TF binding enrichment analysis for p63-dependently regulated genes using Enrichr (Kuleshov et al., 2016). In agreement with its established roles, we identify cell cycle gene regulators (E2F4, E2F6, SIN3A, E2F1, FOXM1, NFYA, and NFYB (Fischer and Müller, 2017)) and the MYC/MAX TFs as being enriched among p63-upregulated genes. Consistent with previous reports, our analysis also identifies KLF4 (Sen et al., 2012) and SMAD4 (Calleja et al., 2016) as potential mediators of p63-dependent gene regulation. In addition, our analysis reveals that androgen receptor (AR), its co-factor ZMIZ1, as well as SP1, FLI1, and NANOG are novel candidates for mediating the p63-dependent up-regulation of multiple genes. Surprisingly, our analysis identified only SOX2 as a frequent binder of genes

down-regulated by p63 (Figure 3A). Consistent with the strong association of p63 up-regulated genes with the cell cycle (Figure 2A) and with cell cycle regulators (Figure 3A), we find that p63 up-regulated genes enrich DREAM (dimerization partner, RB-like, E2F, and multi-vulval class B) and E2F target genes (Figure 3B), and DREAM target genes appear to be modestly but consistently down-regulated when p63 is lost (Figure 3C). Notably, when DREAM targets were already down-regulated through Nutlin treatment in MCF10A cells, loss of p63 decreased their expression even further (Figure 3C) (Karsli Uzunbas et al., 2019), which indicates a possible cumulative effect that is independent of p53 regulatory functions as has been suggested previously (McDade et al., 2014).

Together, the meta-analysis approach overcomes the limitations of individual studies and identifies target genes supported by multiple datasets. The extensive and integrated resource on p63-regulated genes enables researchers to compare their results quickly and to identify the most promising targets.

p63 and p53 regulate largely distinct gene sets

Given that p63 and p53 share a significant number of binding sites and thus potential target genes, we next compared the *p63 Expression Score* to the previously established *p53 Expression Score* (Fischer et al., 2016a). In agreement with the up-regulation of cell cycle genes and DREAM targets through p63 (Figure 2A and 3) and their down-regulation through p53 (Fischer et al., 2016a, 2016b; Schade et al., 2019; Uxa et al., 2019), we noted that negative *p53 Expression Scores* tend to correlate with positive *p63 Expression Scores* (Figure 4A). Furthermore, the results indicate that p53-induced genes (positive *p53 Expression Scores*) appear to be largely unaffected by p63. Consistently, expression data for 346 target genes with strong evidence for direct up-regulation by p53, do not show consistent expression changes upon knockdown or induction of p63 (Figure 4B). Together, these results indicate that basal expression of the majority of p53 target genes is not affected by p63.

Common and distinct properties of p63 and p53 DNA binding

To identify shared p63 and p53 bound sites, we compared the 20 p63 ChIP-seq datasets (Supplementary Table 1) to 28 p53 ChIP-seq datasets we compiled recently (Fischer, 2019). While the majority of all p53 ChIP-seq peaks occurs in only one of the experiments, more than half of the p63 peaks are present in two or more datasets (Figure 5A and B). Even though we were able to integrate substantially more p53 datasets, the number of identified p63 binding sites was still higher (Figure 5C). This indicates that p63 occupies many more binding sites as compared to p53. Importantly, when more datasets agree on p53 and p63 binding sites, these sequences are more likely to harbor a canonical p53 and p63RE, facilitating the motif discovery by tools such as HOMER (Heinz et al., 2010) and enriching *bona fide* binding

sites (Figure 5D). Earlier meta-analyses employed a similar strategy (Fischer et al., 2016a; Nguyen et al., 2018; Verfaillie et al., 2016). To dissect the binding preferences of p63 and p53, we generated three distinct peak sets (Figure 5E). The 'p53+p63' set contained all binding sites with evidence in at least five p63 and five p53 ChIP-seq datasets. The 'p53 unique' (hereafter 'p53') set contained all binding sites that were supported by at least five p53 ChIP-seq datasets but not a single p63 dataset. We also generated a 'p63 unique' (hereafter 'p63') set *vice versa*.

We employed an iterative *de novo* motif search using HOMER to identify frequent binding site motifs. After each round, we removed all peaks harboring the best motif and repeated the search. We identified similar yet distinct binding motifs for the three groups (Figure 5F). Comparison of the primary 'p53+p63', 'p53' and 'p63' suggests that p63 binding sites display a highly conserved C, G, C and G at positions 4, 7, 14 and 17, respectively. The second round reveals a p53RE containing a 1bp spacer (p53 secondary motif), supporting a previously published model that p53 can bind to spacer-containing p53REs (Vyas et al., 2017). The results further indicate that p53 can bind to a single half-site (p53 tertiary motif) and that this single half-site is more constrained at positions 5 and 6 as well as the flanking regions than half-sites in the canonical p53RE (e.g. primary p53+p63 and p53 motifs). Of note, these single half-sites may also include p53REs with spacers longer than 1 bp that are not detected separately because of their very low abundance. Sole half-sites together with spacer-containing p53REs underlie only ~5 % of p53 bound sites (Figure 6). Furthermore, p53 and p63 appear to be able to bind to three-quarter sites (secondary and quaternary p53+p63 and p63 motifs) while p63 can generally bind to a broader spectrum of sequences as compared to p53 (Figure 5F).

It is important to note that the vast majority (~70 %) of p53 and p63 binding sites harbor full-length p53 and p63REs (Figure 6 and 7, Supplementary Table S3). There is a good correlation between p53 and p63 binding site occupation, and most sites commonly bound by p53 are also frequently bound by p63 (Supplementary Figure 1A). However, p63 binds many sites that are not bound by p53 (Supplementary Figure 1B). More importantly, p53 binding is strongly constrained to canonical p53RE (Supplementary Figures 1C-D and 2A-C). In contrast, p63 binding appears not to benefit from a more canonical p63RE (Supplementary Figures 1E-F and 2D-F). These data suggest that sequence-specific binding is particularly important to recruit p53, while p63 only requires minimal sequence identity and could require additional co-factors to bind and ultimately regulate its target genes.

Therefore, we also searched for potential cooperating TFs that may be co-enriched at p53 and p63 binding sites. Consistent with earlier analyses (Verfaillie et al., 2016), no additional motif was substantially enriched in the vicinity of 'p53' or 'p53+p63' binding sites. Consistent with the co-enrichment of AP-1 and p63 at enhancers (Lin-Shiao et al., 2018), we

found that unique p63 binding sites were consistently enriched for AP-1 (bZIP) in addition to bHLH motifs (Supplementary Figure 3). Using the CistromeDB toolkit (Zheng et al., 2019b), we identified TFs that significantly enrich for binding to the 'p53+p63', 'p53', and 'p63' sites. As expected, the analysis identified the p53 family members p53, p63, and p73 as best hits for the common sites, but only p53 and p73 for the unique p53 and only p63 and p73 for the unique p63 peak sets (Supplementary Figure 4). In agreement with earlier studies, the analysis identified p300 (Katoh et al., 2019), MAF (Lopez-Pajares et al., 2015), SOX2 (Watanabe et al., 2014), BANF1 (also known as BAF) (Bao et al., 2015), and KMT2D (Lin-Shiao et al., 2018) as potential co-binders of p63; as well as TRIM28 (Doyle et al., 2010), BRD4 (Stewart et al., 2013), p300 (Lill et al., 1997), ZBTB33 (KAISO) (Koh et al., 2014), CDK9 (Claudio et al., 2006), and HEXIM1 (Lew et al., 2012) as potential co-binders of p53. Moreover, our analysis identified potential co-binders that to our knowledge have not been identified before, such as KDM1A, PRMT1, and GRHL2 for p63 and BRD9, ZNF131, and C17orf49 for p53. Importantly, these new potential co-binders appear to be unique to either p63 or p53, suggesting that they may contribute to shaping the DNA binding landscapes that are specific to p63 and p53 (Supplementary Figure 4).

Identification of direct p63 target genes

Given that p63 regulates many target genes through enhancers (Kouwenhoven et al., 2015a; Lin-Shiao et al., 2018, 2019; Qu et al., 2018; Somerville et al., 2018), straight forward integration of differential gene regulation data and p63 binding data based on proximity binding to a gene's TSS is unlikely to capture all direct p63 target genes. To resolve this issue, we integrated the p63 binding data and the *p63 Expression Score* based on enhancer:gene association information (Fishilevich et al., 2017) in addition to proximity binding to TSSs to predict direct p63 target genes. Given the large number of p63 binding sites identified (Figure 5C and 5E) and the high variance in p63-dependent gene regulation (Figure 1B), we employed conservative thresholds to identify high-probability target genes of p63. We only used p63 binding sites supported by at least half of the datasets (≥10) that are linked through TSS proximity (within 5 kb) or double-elite enhancer:gene associations (Fishilevich et al., 2017) to genes with a |*p63 Expression Score*| ≥ 8 (Figure 8). The 180 (138 up-regulated and 42 down-regulated) genes that passed our conservative filtering contain many genes that are known direct p63 targets, such as *RAB38* (Barton et al., 2010), *S100A2* (Kirschner et al., 2008), *HAS3* (Compagnone et al., 2017), *IRF6* (Thomason et al., 2010), *PTHLH* (Somerville et al., 2018), *GPX2* (Yan and Chen, 2006), *JAG1* (Sasaki et al., 2002), *MMP14* (Lodillinsky et al., 2016), *NRG1* (Forster et al., 2014), and *PLAC8* (Gallant-Behm et al., 2012). The identification of these well-established p63 target genes indicates the ability of our approach to identify *bona fide* candidates. Importantly, the integration of enhancer:gene associations enabled the

identification of genes that are likely regulated by p63 through enhancers, such as *IL1B*, *MREG*, *MYO5A*, *RRP12*, *SNCA*, *AK4*, and *EHD4* (Figure 8).

A p63/SCC 28-gene signature correlates with HNSC patient survival

Out of the 180 high-probability p63 target genes 32 (28 up- and 4 down-regulated) are also identified as being commonly up- or down-regulated in SCCs compared to non-SCC cancers (Campbell et al., 2018) (Figure 8). Importantly, several of the genes commonly up-regulated by p63 as well as in SCC have been identified to promote SCC growth or invasion, such as *LAD1* (Abe et al., 2019), *TMEM40* (Zhang et al., 2019), *FGFBP1* (Czubayko et al., 1997), *IL1B* (Lee et al., 2015), *FAT2* (Dang et al., 2016), *FOSL1* (Usui et al., 2012), *LPAR3* (Brusevold et al., 2014), *MMP14* (Pang et al., 2016), and *RASSF6* (Zheng et al., 2019a). Therefore, we asked whether the set of 28 up-regulated direct p63 targets correlates with patient survival. To this end, we employed data of head and neck squamous cell carcinoma (HNSC) patients from The Cancer Genome Atlas (TCGA). Notably, it is known that this cancer type frequently harbors amplified *TP63* (Lawrence et al., 2015). We find that expression levels of our gene set indeed correlate significantly negatively with HNSC patient survival (COX likelihood ratio test p=0.032). To determine whether expression levels of the set have an influence on the survival of HNSC patients, we subdivided the samples according to the average expression levels into four equally sized groups (low, low-med, med-high, high). While the sample group with low expression had the most favorable prognosis, the null hypothesis could not be rejected in the direct comparison with patients with high average expression levels (p=0.090; Figure 9a). However, upon contrasting the low-expression group with all remaining samples, a significant improvement of survival was detected (p=0.024; Figure 9b). Together, these findings indicate that the genes commonly up-regulated by p63 and in SCC influence the prognosis of HNSC patients. Thus, this finding calls for a more detailed assessment of ubiquitous p63/SCC genes as biomarkers in the future.

Discussion

Although p63 (ΔNp63) is known as master regulator in epidermis development and more recently emerged as a key oncogenic factor in SCC, a comprehensive assessment of the GRN commonly controlled by p63 and its comparison to the GRN commonly controlled by the closely related tumor suppressor p53 has been missing. An increasing number of available high-throughput datasets enabled us to generate ranked lists of p63-regulated genes and p63 bound DNA sites that together reveal high-probability direct p63 target genes regulated by p63 across cells of multiple origins. Because p63 target genes, very much like p53 target genes (Fischer, 2019), differ substantially between mouse and human (Sethi et al., 2017), many p63

target genes initially described in mouse could not be confirmed to be p63-regulated in this study using human data. Given that p63 binding sites are frequently associated with enhancer regions and enhancer identity, we have integrated enhancer:gene associations to identify target genes that are regulated by p63 through direct binding to associated enhancers. This approach enabled the identification of novel direct target genes that are missed by standard analyses that employ only TSS proximity (Figure 8).

Given the similarity between their DBDs, it has been a long-standing question how p53 and p63 bind to distinct sites in the genome and how these sites differ from another. Several studies found differences in the biochemical properties of p53 and p63 that could affect their DNA binding specificity (Enthart et al., 2016; Lokshin et al., 2007; Sauer et al., 2008; Tichý et al., 2013). Various studies aimed to identify the precise p63 recognition motif and its difference from the p53RE using either SELEX (Ortt and Sinha, 2006; Perez et al., 2007) or ChIP-seq data (Kouwenhoven et al., 2010; McDade et al., 2014; Yang et al., 2006), yet these studies reported different features as being unique for p63 compared to p53 DNA recognition. By combining multiple ChIP-seq datasets we have contributed here to better distinguish between sites commonly bound by p53 and p63 across cell types and sites that are unique to p53 or p63 (Figure 5E). Most importantly, our results could explain why a substantial fraction of DNA sites is occupied exclusively by p53 or p63. While most sites bound by p53 are also commonly occupied by p63 (Figure 5E and Supplementary Figure 1A), single half-sites and half-sites separated by spacers underlie many sites that are only bound by p53 (Figure 5F and 6), supporting earlier findings whereby p53 can be recruited through spacer-containing motifs (Vyas et al., 2017). However, while spacers reportedly have been identified in fifty percent of 200 analyzed p53REs (Vyas et al., 2017), our genome-wide quantification of motifs underlying 7705 high confidence p53 peaks based on an unbiased motif search using HOMER revealed that only 1.1 to 5.1% of the p53 peaks contain p53REs with 1 bp spacers or half sites that are possibly separated by longer spacers (Figure 6). Mechanistically, our results imply that relying on the CWWG core motif and the flanking regions may enable p53 to bind to those sites. In contrast, the two CNNG core motifs that underlie p63, but not p53REs, offer an explanation why a substantial fraction of DNA sites is bound exclusively by p63 (Figure 5F and 7), supporting one of the models established earlier (McDade et al., 2014). In addition, our motif search indicates that factors bound to AP-1 (bZIP) and bHLH motifs may specifically support p63 binding (Supplementary Figure 3), and transcription factor enrichment analysis identified the bZIP TF MAF, the TF GRHL2, the chromatin remodeler BANF1, the histone methyltransferase PRMT1, and the ZNF750/KDM1A/KLF4 complex, which was previously shown to operate downstream of p63 (Boxer et al., 2014), as potential co-binders that could help to facilitate p63 binding to certain genomic loci (Supplementary Figure 4). Considering its pioneer role, p63 could *vice versa* enable the binding of these TFs to the respective loci. Given

that p63 and p73 form stable heterotetramers (Gebel et al., 2016), p73 may possess binding specificities that are highly similar to those identified for p63. Our results indicate that our approach could serve as a blueprint to distinguish DNA recognition motifs, binding sites, co-factors, and target genes of TF siblings more precisely. Our iterative *de novo* search algorithm enabled the identification of spacer-containing p53REs, indicating that our approach uncovers second-tier TF binding motifs invisible to standard approaches. Moreover, the results provide insights to the p63 DNA binding repertoire in unprecedented depth (Figure 5F).

Consistent with results from an earlier genome-wide study (Yang et al., 2006), our findings imply that p63 is more frequently involved in a direct up-regulation as opposed to a direct down-regulation of target genes (Figure 3A and 8). Mechanistically, p63 has been shown to up-regulate target genes through its alternative TAD located at the N-terminus while the C-terminus is important for down-regulation (Helton et al., 2006). Exogenous expression of different isoforms of p53 family members and their antagonistic effects on target gene promoters in luciferase reporter assays suggested a model whereby p63 exhibits a dominant negative effect on other p53 family members (Mundt et al., 2010; Westfall et al., 2003; Yang et al., 1998). Inconsistent with its reputation as dominant negative regulator of p53, however, genome-wide studies showed that the groups of p63-regulated genes and p53-regulated genes show only very little overlap (Gallant-Behm et al., 2012). A recent analysis of DNA sites bound and of genes regulated by p53 and p63 revealed that p63 is more likely to support than to inhibit p53 activity (Karsli Uzunbas et al., 2019). Our analysis further supports the notion that p63 does not commonly interfere with target gene up-regulation by p53 but that except for cell cycle genes they regulate largely distinct gene sets (Figure 4).

We identify several candidate TFs that may operate downstream of p63 and that may serve as transitional nodes in the p63 GRN. In addition to known mediators of p63-dependent gene regulation, such as MYC and KLF4, we identify AR and its co-factor ZMIZ1, SP1, FLI1, and NANOG as novel candidate nodes in the p63 GRN (Figure 3A). In agreement with the tumor suppressor role of p53 and the oncogenic role of p63, we find that cell cycle genes are antagonistically regulated by p53 and p63 (Figure 2A and 4A). On the one hand, cell cycle genes are well-known to be down-regulated by p53 indirectly through the cyclin-dependent kinase inhibitor p21 and the cell cycle repressor complexes DREAM and RB-E2F (Fischer et al., 2016a, 2016b; Schade et al., 2019; Uxa et al., 2019). On the other hand, cell cycle genes are down-regulated upon loss of p63 and this p63-dependent regulation reportedly occurs through regulating p21 signaling and the DREAM component p130 (McDade et al., 2011; Truong et al., 2006). In addition to indirect effects, we also identified multiple cell cycle genes as high-probability direct p63 targets (Figure 8). Thus, p63 appears to directly drive the expression of some cell cycle genes and to indirectly up-regulate the whole set of cell cycle genes through affecting the function of cell cycle regulators. While the up-regulation of cell

cycle genes occurs in most cancers (Whitfield et al., 2006), we find that p63 additionally regulates genes that are specifically altered across SCCs (Figure 2D). These results underscore the critical role of p63 and its target genes in determining the transcriptional profile of SCC. An example of a p63 target in SCC is NRG1, which can be inhibited to block SCC proliferation and tumor growth (Hegde et al., 2019). The resource of genes commonly regulated by p63 provided here may help to identify targets that can be exploited therapeutically. Expression levels of the 28 p63 target genes that are commonly up-regulated by p63 and in SCC (Figure 8) correlate significantly with poorer survival of HNSC patients (Figure 9). This 28-gene set may contain particularly promising candidates for therapeutic interventions and for the use as biomarkers.

Methods

Re-analysis and integration of publicly available gene expression profiling datasets

We re-analyzed publicly available p63-dependent gene expression profiling datasets. As a first quality requirement, we only included datasets for re-analysis that contained at least two biological replicates for the treatment as well as for the control condition. All microarray datasets were available at a pre-processed stage at the Gene Expression Omnibus (GEO) and we re-analyzed these datasets with GEO2R to obtain fold expression changes and Benjamini Hochberg-corrected p-values (Clough and Barrett, 2016). Gene identifiers were mapped to Ensembl Gene IDs using the Ensembl annotation data (Cunningham et al., 2019). All RNA-seq datasets have been retrieved through GEO from the Sequence Read Archive (SRA) (Leinonen et al., 2011). We employed our RNA-seq analysis pipeline to obtain fold expression changes and p-values adjusted for multiple testing. Briefly, we utilized Trimmomatic (Bolger et al., 2014) v0.39 (5nt sliding window approach, mean quality cutoff 22) for read quality trimming according to inspections made from FastQC (https://www.bioinformatics.babraham.ac.uk/projects/fastqc/) v0.11.8 reports. Clipping was performed using Cutadapt v2.3 (Martin, 2011). Potential sequencing errors were detected and corrected using Rcorrector v1.0.3.1 (Song and Florea, 2015). Ribosomal RNA (rRNA) transcripts were artificially depleted by read alignment against rRNA databases through SortMeRNA v2.1 (Kopylova et al., 2012). The preprocessed data was aligned to the reference genome hg38, retrieved along with its gene annotation from Ensembl v.92 (Cunningham et al., 2019). For read alignment, we used the splice-aware mapping software segemehl (Hoffmann et al., 2009, 2014) v0.3.4 with adjusted accuracy (95%). Mappings were filtered by Samtools v1.9 (Li et al., 2009) for uniqueness and properly aligned mate pairs. Read quantification was performed on exon level using featureCounts v1.6.5 (Liao et al., 2014), parametrized according to the strand specificity inferred through RSeQC v3.0.0 (Wang et al., 2012). Differential gene expression and its statistical significance was identified using DESeq2 v1.20.0 (Love et al., 2014). Information on the samples that were compared for each dataset is included in Supplementary Table 1. Given that all RNA-seq data was derived from PolyA-enriched samples, we only included Ensembl transcript types ‘protein_coding’, ‘antisense’, ‘lincRNA’ and ‘TEC’ in our analysis. Common thresholds for adj. p-value ≤ 0.05 were applied.

Generation of the p63 Expression Score

For 19,156 genes covered by at least three datasets including a minimum of one RNA-seq dataset, a *p63 Expression Score* was calculated as the number of datasets that find the gene to be significantly up-regulated minus the number of datasets that find the gene to be significantly down-regulated in dependence on p63. This meta-analysis resulted in 27 *p63*

Expression Score gene groups because no gene was identified as up-regulated in all 16 or 15 datasets or down-regulated in all 16, 15, 14 or 13 datasets.

Gene set enrichment analysis (GSEA)

Gene set enrichment analysis was performed using GSEA (http://software.broadinstitute.org/gsea/) with 'H', 'C2', and 'C6' gene sets from MSigDB v7.0 (Subramanian et al., 2005) and custom panSCC gene sets derived from Table S1C in Campbell *et al.* (Campbell et al., 2018). GSEA was performed on a pre-ranked list of genes that were ranked primarily by *p63 Expression Score* and secondarily by median $\log_2$(fold-change) to obtain unique ranks.

Integration of publicly available p63 and p53 binding data

Peak datasets from p63 ChIP-seq experiments were retrieved from CistromeDB (Zheng et al., 2019b) (Supplementary Table 1). When replicate experiments were available, all peaks were used that have been identified in at least two replicates. A similar collection of p53 peak datasets has been described previously (Fischer, 2019). To intersect multiple peak files Bedtools 'multiinter' was used and to identify overlapping and non-overlapping peaks Bedtools 'intersect' was employed (Quinlan and Hall, 2010).

Motif search

Known p53 and p63REs were identified using the 'known motifs' in HOMER v4.10 with default options and *-size given* (Heinz et al., 2010). *De novo* motif discovery was performed with options *-size given -len 10,15,20,25 -mis 5 -S 10*.

Identification of potential co-factors

We used the CistromeDB toolkit (Zheng et al., 2019b) to identify TFs that display ChIP-seq peaksets that are significantly similar to our 'unique p53', 'unique p63', and 'p53+p63' peaksets.

Survival analysis

For the 28-gene set, single-sample enrichment scores were derived from FPKM normalized gene expression values of 546 HNSC patient samples. To this end, we utilized the official GenePattern single sample gene set enrichment analysis (ssGSEA) codebase v10.0.3 (https://github.com/GSEA-MSigDB/ssGSEA-gpmodule). A sample score represents the coordinately up- or down-regulated expression of all genes within one set as its signature (Barbie et al., 2009). Kaplan-Meier plots and correlation analyses were performed on TCGA time to event and event occurrence information using the R survival package v3.2-3. Following

the TCGA standard for HNSC (Lawrence et al., 2015), survival analyses were right-censored at 60 months (1800 days) to avoid non-cancer-related events. The Cox proportional hazards model was used to investigate the association of patient survival time and the combined expression levels of the 28-gene set. Subsequently, we subdivided the expression scores into four equally sized categorical groups (high, med-high, med-low, low). The rates of occurrence of events over time were compared between these groups using the fitted COX PH model.

Author Contributions

MF conceived and supervised the study. MF, SH, KR, HK, and AS designed the analyses. KR, MF, and HK performed the analyses. MF, SH, and SSM interpreted the data. MF wrote the initial manuscript draft. All authors edited and approved the manuscript.

Funding

This work was supported through the German Research Foundation (DFG) [FI 1993/2-1 to MF] and the German Federal Ministry for Education and Research (BMBF) [031L016D to SH]. The FLI is a member of the Leibniz Association and is financially supported by the Federal Government of Germany and the State of Thuringia.

Conflicts of interest

The authors declare no conflict of interest.

Reference List

Abe, D.T., Yamazaki, D.M., Maruyama, D.S., and Ajioka, P.Y. (2019). Ladinin-1 is involved in cell motility and proliferation of oral squamous cell carcinoma cells. Oral Surg. Oral Med. Oral Pathol. Oral Radiol. *128*, e81–e82.
Abraham, C.G., Ludwig, M.P., Andrysik, Z., Pandey, A., Joshi, M., Galbraith, M.D., Sullivan, K.D., and Espinosa, J.M. (2018). ΔNp63α Suppresses TGFB2 Expression and RHOA Activity to Drive Cell Proliferation in Squamous Cell Carcinomas. Cell Rep. *24*, 3224–3236.
Bao, X., Rubin, A.J., Qu, K., Zhang, J., Giresi, P.G., Chang, H.Y., and Khavari, P.A. (2015). A novel ATAC-seq approach reveals lineage-specific reinforcement of the open chromatin landscape via cooperation between BAF and p63. Genome Biol. *16*, 284.
Barbie, D.A., Tamayo, P., Boehm, J.S., Kim, S.Y., Moody, S.E., Dunn, I.F., Schinzel, A.C., Sandy, P., Meylan, E., Scholl, C., et al. (2009). Systematic RNA interference reveals that oncogenic KRAS-driven cancers require TBK1. Nature *462*, 108–112.
Barton, C.E., Johnson, K.N., Mays, D.M., Boehnke, K., Shyr, Y., Boukamp, P., and Pietenpol, J.A. (2010). Novel p63 target genes involved in paracrine signaling and keratinocyte differentiation. Cell Death Dis. *1*, e74.
Bolger, A.M., Lohse, M., and Usadel, B. (2014). Trimmomatic: a flexible trimmer for Illumina sequence data. Bioinformatics *30*, 2114–2120.
Boxer, L.D., Barajas, B., Tao, S., Zhang, J., and Khavari, P.A. (2014). Znf750 interacts with

KLF4 and RCOR1, KDM1A, And CTBP1/2 chromatin regulators to repress epidermal progenitor genes and induce differentiation genes. Genes Dev. *28*, 2013–2026.
Brusevold, I.J., Tveteraas, I.H., Aasrum, M., Ødegård, J., Sandnes, D.L., and Christoffersen, T. (2014). Role of LPAR3, PKC and EGFR in LPA-induced cell migration in oral squamous carcinoma cells. BMC Cancer *14*.
Calleja, L.R., Jacques, C., Lamoureux, F., Baud'Huin, M., Gabriel, M.T., Quillard, T., Sahay, D., Perrot, P., Amiaud, J., Charrier, C., et al. (2016). ΔNp63α silences a miRNA program to aberrantly initiate a wound-healing program that promotes TGFβ-induced metastasis. Cancer Res. *76*, 3236–3251.
Campbell, J.D., Yau, C., Bowlby, R., Liu, Y., Brennan, K., Fan, H., Taylor, A.M., Wang, C., Walter, V., Akbani, R., et al. (2018). Genomic, Pathway Network, and Immunologic Features Distinguishing Squamous Carcinomas. Cell Rep. *23*, 194-212.e6.
Carroll, D.K., Carroll, J.S., Leong, C.-O., Cheng, F., Brown, M., Mills, A.A., Brugge, J.S., and Ellisen, L.W. (2006). p63 regulates an adhesion programme and cell survival in epithelial cells. Nat. Cell Biol. *8*, 551–561.
Chakrabarti, R., Wei, Y., Hwang, J., Hang, X., Andres Blanco, M., Choudhury, A., Tiede, B., Romano, R.A., Decoste, C., Mercatali, L., et al. (2014). Δnp63 promotes stem cell activity in mammary gland development and basal-like breast cancer by enhancing Fzd7 expression and Wnt signalling. Nat. Cell Biol. *16*, 1004–1015.
Claudio, P.P., Cui, J., Ghafouri, M., Mariano, C., White, M.K., Safak, M., Sheffield, J.B., Giordano, A., Khalili, K., Amini, S., et al. (2006). Cdk9 phosphorylates p53 on serine 392 independently of CKII. J. Cell. Physiol. *208*, 602–612.
Clough, E., and Barrett, T. (2016). The Gene Expression Omnibus Database. Methods Mol. Biol. *1418*, 93–110.
Compagnone, M., Gatti, V., Presutti, D., Ruberti, G., Fierro, C., Markert, E.K., Vousden, K.H., Zhou, H., Mauriello, A., Anemone, L., et al. (2017). ΔNp63-mediated regulation of hyaluronic acid metabolism and signaling supports HNSCC tumorigenesis. Proc. Natl. Acad. Sci. *114*, 13254–13259.
Cunningham, F., Achuthan, P., Akanni, W., Allen, J., Amode, M.R., Armean, I.M., Bennett, R., Bhai, J., Billis, K., Boddu, S., et al. (2019). Ensembl 2019. Nucleic Acids Res. *47*, D745–D751.
Czubayko, F., Liaudet-Coopman, E.D.E., Aigner, A., Tuveson, A.T., Berchem, G.J., and Wellstein, A. (1997). A secreted FGF-binding protein can serve as the angiogenic switch in human cancer. Nat. Med. *3*, 1137–1140.
Dang, T.T., Westcott, J.M., Maine, E.A., Kanchwala, M., Xing, C., and Pearson, G.W. (2016). ΔNp63α induces the expression of FAT2 and Slug to promote tumor invasion. Oncotarget *7*, 28592–28611.
Doyle, J.M., Gao, J., Wang, J., Yang, M., and Potts, P.R. (2010). MAGE-RING protein complexes comprise a family of E3 ubiquitin ligases. Mol. Cell *39*, 963–974.
Enthart, A., Klein, C., Dehner, A., Coles, M., Gemmecker, G., Kessler, H., and Hagn, F. (2016). Solution structure and binding specificity of the p63 DNA binding domain. Sci. Rep. *6*, 26707.
Fischer, M. (2017). Census and evaluation of p53 target genes. Oncogene *36*, 3943–3956.
Fischer, M. (2019). Conservation and divergence of the p53 gene regulatory network between mice and humans. Oncogene *38*, 4095–4109.
Fischer, M., and Müller, G.A. (2017). Cell cycle transcription control: DREAM/MuvB and RB-E2F complexes. Crit. Rev. Biochem. Mol. Biol. *52*, 638–662.
Fischer, M., Steiner, L., and Engeland, K. (2014). The transcription factor p53: Not a repressor, solely an activator. Cell Cycle *13*, 3037–3058.
Fischer, M., Grossmann, P., Padi, M., and DeCaprio, J.A. (2016a). Integration of TP53, DREAM, MMB-FOXM1 and RB-E2F target gene analyses identifies cell cycle gene regulatory networks. Nucleic Acids Res. *44*, 6070–6086.
Fischer, M., Quaas, M., Steiner, L., and Engeland, K. (2016b). The p53-p21-DREAM-CDE/CHR pathway regulates G2/M cell cycle genes. Nucleic Acids Res. *44*, 164–174.
Fischer, M., Uxa, S., Stanko, C., Magin, T.M., and Engeland, K. (2017). Human papilloma virus E7 oncoprotein abrogates the p53-p21-DREAM pathway. Sci. Rep. *7*, 2603.

Fishilevich, S., Nudel, R., Rappaport, N., Hadar, R., Plaschkes, I., Iny Stein, T., Rosen, N., Kohn, A., Twik, M., Safran, M., et al. (2017). GeneHancer: genome-wide integration of enhancers and target genes in GeneCards. Database (Oxford). *2017*.
Forster, N., Saladi, S.V., van Bragt, M., Sfondouris, M.E., Jones, F.E., Li, Z., and Ellisen, L.W. (2014). Basal Cell Signaling by p63 Controls Luminal Progenitor Function and Lactation via NRG1. Dev. Cell *28*, 147–160.
Gallant-Behm, C.L., Ramsey, M.R., Bensard, C.L., Nojek, I., Tran, J., Liu, M., Ellisen, L.W., and Espinosa, J.M. (2012). ΔNp63α represses anti-proliferative genes via H2A.Z deposition. Genes Dev. *26*, 2325–2336.
Gatti, V., Fierro, C., Annicchiarico-Petruzzelli, M., Melino, G., and Peschiaroli, A. (2019). ΔNp63 in squamous cell carcinoma: defining the oncogenic routes affecting epigenetic landscape and tumour microenvironment. Mol. Oncol. *13*, 1878-0261.12473.
Gebel, J., Luh, L.M., Coutandin, D., Osterburg, C., Löhr, F., Schäfer, B., Frombach, A.-S., Sumyk, M., Buchner, L., Krojer, T., et al. (2016). Mechanism of TAp73 inhibition by ΔNp63 and structural basis of p63/p73 hetero-tetramerization. Cell Death Differ. *23*, 1930–1940.
Hegde, G. V, de la Cruz, C., Giltnane, J.M., Crocker, L., Venkatanarayan, A., Schaefer, G., Dunlap, D., Hoeck, J.D., Piskol, R., Gnad, F., et al. (2019). NRG1 is a critical regulator of differentiation in TP63-driven squamous cell carcinoma. Elife *8*.
Heinz, S., Benner, C., Spann, N., Bertolino, E., Lin, Y.C., Laslo, P., Cheng, J.X., Murre, C., Singh, H., and Glass, C.K. (2010). Simple combinations of lineage-determining transcription factors prime cis-regulatory elements required for macrophage and B cell identities. Mol. Cell *38*, 576–589.
Helton, E.S., Zhu, J., and Chen, X. (2006). The unique NH2-terminally deleted (DeltaN) residues, the PXXP motif, and the PPXY motif are required for the transcriptional activity of the DeltaN variant of p63. J. Biol. Chem. *281*, 2533–2542.
Hoffmann, S., Otto, C., Kurtz, S., Sharma, C.M., Khaitovich, P., Vogel, J., Stadler, P.F., and Hackermüller, J. (2009). Fast Mapping of Short Sequences with Mismatches, Insertions and Deletions Using Index Structures. PLoS Comput. Biol. *5*, e1000502.
Hoffmann, S., Otto, C., Doose, G., Tanzer, A., Langenberger, D., Christ, S., Kunz, M., Holdt, L.M., Teupser, D., Hackermüller, J., et al. (2014). A multi-split mapping algorithm for circular RNA, splicing, trans-splicing and fusion detection. Genome Biol. *15*, R34.
Karsli Uzunbas, G., Ahmed, F., and Sammons, M.A. (2019). Control of p53-dependent transcription and enhancer activity by the p53 family member p63. J. Biol. Chem. *294*, 10720–10736.
Katoh, I., Maehata, Y., Moriishi, K., Hata, R.I., and Kurata, S. ichi (2019). C-terminal α Domain of p63 Binds to p300 to Coactivate β-Catenin. Neoplasia (United States) *21*, 494–503.
King, K.E., Ponnamperuma, R.M., Yamashita, T., Tokino, T., Lee, L.A., Young, M.F., and Weinberg, W.C. (2003). deltaNp63alpha functions as both a positive and a negative transcriptional regulator and blocks in vitro differentiation of murine keratinocytes. Oncogene *22*, 3635–3644.
Kirschner, R.D., Sänger, K., Müller, G.A., and Engeland, K. (2008). Transcriptional activation of the tumor suppressor and differentiation gene S100A2 by a novel p63-binding site. Nucleic Acids Res. *36*, 2969–2980.
Kitayner, M., Rozenberg, H., Rohs, R., Suad, O., Rabinovich, D., Honig, B., and Shakked, Z. (2010). Diversity in DNA recognition by p53 revealed by crystal structures with Hoogsteen base pairs. Nat. Struct. Mol. Biol. *17*, 423–429.
Koh, D.I., Han, D., Ryu, H., Choi, W. Il, Jeon, B.N., Kim, M.K., Kim, Y., Kim, J.Y., Parry, L., Clarke, A.R., et al. (2014). KAISO, a critical regulator of p53-mediated transcription of CDKN1A and apoptotic genes. Proc. Natl. Acad. Sci. U. S. A. *111*, 15078–15083.
Kopylova, E., Noé, L., and Touzet, H. (2012). SortMeRNA: Fast and accurate filtering of ribosomal RNAs in metatranscriptomic data. Bioinformatics *28*, 3211–3217.
Kouwenhoven, E.N., van Heeringen, S.J., Tena, J.J., Oti, M., Dutilh, B.E., Alonso, M.E., de la Calle-Mustienes, E., Smeenk, L., Rinne, T., Parsaulian, L., et al. (2010). Genome-Wide Profiling of p63 DNA–Binding Sites Identifies an Element that Regulates Gene Expression during Limb Development in the 7q21 SHFM1 Locus. PLoS Genet. *6*, e1001065.

Kouwenhoven, E.N., Oti, M., Niehues, H., van Heeringen, S.J., Schalkwijk, J., Stunnenberg, H.G., Bokhoven, H., and Zhou, H. (2015a). Transcription factor p63 bookmarks and regulates dynamic enhancers during epidermal differentiation. EMBO Rep. *16*, 863–878.
Kouwenhoven, E.N., van Bokhoven, H., and Zhou, H. (2015b). Gene regulatory mechanisms orchestrated by p63 in epithelial development and related disorders. Biochim. Biophys. Acta - Gene Regul. Mech. *1849*, 590–600.
Kuleshov, M. V., Jones, M.R., Rouillard, A.D., Fernandez, N.F., Duan, Q., Wang, Z., Koplev, S., Jenkins, S.L., Jagodnik, K.M., Lachmann, A., et al. (2016). Enrichr: a comprehensive gene set enrichment analysis web server 2016 update. Nucleic Acids Res. *44*, W90–W97.
Lawrence, M.S., Sougnez, C., Lichtenstein, L., Cibulskis, K., Lander, E., Gabriel, S.B., Getz, G., Ally, A., Balasundaram, M., Birol, I., et al. (2015). Comprehensive genomic characterization of head and neck squamous cell carcinomas. Nature *517*, 576–582.
Lee, C.H., Chang, J.S.M., Syu, S.H., Wong, T.S., Chan, J.Y.W., Tang, Y.C., Yang, Z.P., Yang, W.C., Chen, C.T., Lu, S.C., et al. (2015). IL-1β promotes malignant transformation and tumor aggressiveness in oral cancer. J. Cell. Physiol. *230*, 875–884.
Leinonen, R., Sugawara, H., Shumway, M., and International Nucleotide Sequence Database Collaboration (2011). The sequence read archive. Nucleic Acids Res. *39*, D19-21.
Lew, Q.J., Chia, Y.L., Chu, K.L., Lam, Y.T., Gurumurthy, M., Xu, S., Lam, K.P., Cheong, N., and Chao, S.H. (2012). Identification of HEXIM1 as a positive regulator of p53. J. Biol. Chem. *287*, 36443–36454.
Li, H., Handsaker, B., Wysoker, A., Fennell, T., Ruan, J., Homer, N., Marth, G., Abecasis, G., and Durbin, R. (2009). The Sequence Alignment/Map format and SAMtools. Bioinformatics *25*, 2078–2079.
Liao, Y., Smyth, G.K., and Shi, W. (2014). FeatureCounts: An efficient general purpose program for assigning sequence reads to genomic features. Bioinformatics *30*, 923–930.
Lill, N.L., Grossman, S.R., Ginsberg, D., DeCaprio, J., and Livingston, D.M. (1997). Binding and modulation of p53 by p300/CBP coactivators. Nature *387*, 823–827.
Lin-Shiao, E., Lan, Y., Coradin, M., Anderson, A., Donahue, G., Simpson, C.L., Sen, P., Saffie, R., Busino, L., Garcia, B.A., et al. (2018). KMT2D regulates p63 target enhancers to coordinate epithelial homeostasis. Genes Dev. *32*, 181–193.
Lin-Shiao, E., Lan, Y., Welzenbach, J., Alexander, K.A., Zhang, Z., Knapp, M., Mangold, E., Sammons, M., Ludwig, K.U., and Berger, S.L. (2019). p63 establishes epithelial enhancers at critical craniofacial development genes. Sci. Adv. *5*, eaaw0946.
Lin, Y.-L., Sengupta, S., Gurdziel, K., Bell, G.W., Jacks, T., and Flores, E.R. (2009). p63 and p73 transcriptionally regulate genes involved in DNA repair. PLoS Genet. *5*, e1000680.
Lodillinsky, C., Infante, E., Guichard, A., Chaligné, R., Fuhrmann, L., Cyrta, J., Irondelle, M., Lagoutte, E., Vacher, S., Bonsang-Kitzis, H., et al. (2016). p63/MT1-MMP axis is required for in situ to invasive transition in basal-like breast cancer. Oncogene *35*, 344–357.
Lokshin, M., Li, Y., Gaiddon, C., and Prives, C. (2007). p53 and p73 display common and distinct requirements for sequence specific binding to DNA. Nucleic Acids Res. *35*, 340–352.
Lopez-Pajares, V., Qu, K., Zhang, J., Webster, D.E., Barajas, B.C., Siprashvili, Z., Zarnegar, B.J., Boxer, L.D., Rios, E.J., Tao, S., et al. (2015). A LncRNA-MAF:MAFB transcription factor network regulates epidermal differentiation. Dev. Cell *32*, 693–706.
Love, M.I., Huber, W., and Anders, S. (2014). Moderated estimation of fold change and dispersion for RNA-seq data with DESeq2. Genome Biol. *15*, 550.
Martin, M. (2011). Cutadapt removes adapter sequences from high-throughput sequencing reads. EMBnet.Journal *17*, 10.
McDade, S.S., Patel, D., and McCance, D.J. (2011). p63 maintains keratinocyte proliferative capacity through regulation of Skp2-p130 levels. J. Cell Sci. *124*, 1635–1643.
McDade, S.S., Henry, A.E., Pivato, G.P., Kozarewa, I., Mitsopoulos, C., Fenwick, K., Assiotis, I., Hakas, J., Zvelebil, M., Orr, N., et al. (2012). Genome-wide analysis of p63 binding sites identifies AP-2 factors as co-regulators of epidermal differentiation. Nucleic Acids Res. *40*, 7190–7206.
McDade, S.S., Patel, D., Moran, M., Campbell, J., Fenwick, K., Kozarewa, I., Orr, N.J., Lord, C.J., Ashworth, A.A., and McCance, D.J. (2014). Genome-wide characterization reveals complex interplay between TP53 and TP63 in response to genotoxic stress. Nucleic Acids

Res. *42*, 6270–6285.
Mehta, S.Y., Morten, B.C., Antony, J., Henderson, L., Lasham, A., Campbell, H., Cunliffe, H., Horsfield, J.A., Reddel, R.R., Avery-Kiejda, K.A., et al. (2018). Regulation of the interferon-gamma (IFN-γ) pathway by p63 and Δ133p53 isoform in different breast cancer subtypes. Oncotarget *9*, 29146–29161.
Menendez, D., Nguyen, T.A., Freudenberg, J.M., Mathew, V.J., Anderson, C.W., Jothi, R., and Resnick, M.A. (2013). Diverse stresses dramatically alter genome-wide p53 binding and transactivation landscape in human cancer cells. Nucleic Acids Res. *41*, 7286–7301.
Mills, A.A., Zheng, B., Wang, X.J., Vogel, H., Roop, D.R., and Bradley, A. (1999). P63 Is a P53 Homologue Required for Limb and Epidermal Morphogenesis. Nature *398*, 708–713.
Mundt, H.M., Stremmel, W., Melino, G., Krammer, P.H., Schilling, T., and Müller, M. (2010). Dominant negative (ΔN) p63α induces drug resistance in hepatocellular carcinoma by interference with apoptosis signaling pathways. Biochem. Biophys. Res. Commun. *396*, 335–341.
Murray-Zmijewski, F., Lane, D.P., and Bourdon, J.-C. (2006). P53/P63/P73 Isoforms: an Orchestra of Isoforms To Harmonise Cell Differentiation and Response To Stress. Cell Death Differ. *13*, 962–972.
Nguyen, T.-A.T., Grimm, S.A., Bushel, P.R., Li, J., Li, Y., Bennett, B.D., Lavender, C.A., Ward, J.M., Fargo, D.C., Anderson, C.W., et al. (2018). Revealing a human p53 universe. Nucleic Acids Res. *46*, 8153–8167.
Ortt, K., and Sinha, S. (2006). Derivation of the consensus DNA-binding sequence for p63 reveals unique requirements that are distinct from p53. FEBS Lett. *580*, 4544–4550.
Pang, L., Li, Q., Li, S., He, J., Cao, W., Lan, J., Sun, B., Zou, H., Wang, C., Liu, R., et al. (2016). Membrane type 1-matrix metalloproteinase induces epithelial-to-mesenchymal transition in esophageal squamous cell carcinoma: Observations from clinical and in vitro analyses. Sci. Rep. *6*.
Perez, C.A., Ott, J., Mays, D.J., and Pietenpol, J.A. (2007). p63 consensus DNA-binding site: identification, analysis and application into a p63MH algorithm. Oncogene *26*, 7363–7370.
Qu, J., Tanis, S.E.J., Smits, J.P.H., Kouwenhoven, E.N., Oti, M., van den Bogaard, E.H., Logie, C., Stunnenberg, H.G., van Bokhoven, H., Mulder, K.W., et al. (2018). Mutant p63 Affects Epidermal Cell Identity through Rewiring the Enhancer Landscape. Cell Rep. *25*, 3490-3503.e4.
Quinlan, A.R., and Hall, I.M. (2010). BEDTools: A flexible suite of utilities for comparing genomic features. Bioinformatics *26*, 841–842.
Ramsey, M.R., Wilson, C., Ory, B., Rothenberg, S.M., Faquin, W., Mills, A.A., and Ellisen, L.W. (2013). FGFR2 signaling underlies p63 oncogenic function in squamous cell carcinoma. J. Clin. Invest. *123*, 3525–3538.
Saladi, S.V., Ross, K., Karaayvaz, M., Tata, P.R., Mou, H., Rajagopal, J., Ramaswamy, S., and Ellisen, L.W. (2017). ACTL6A Is Co-Amplified with p63 in Squamous Cell Carcinoma to Drive YAP Activation, Regenerative Proliferation, and Poor Prognosis. Cancer Cell *31*, 35–49.
Sammons, M.A., Nguyen, T.-A.T., McDade, S.S., and Fischer, M. (2020). Tumor suppressor p53: from engaging DNA to target gene regulation. Nucleic Acids Res.
Sasaki, Y., Ishida, S., Morimoto, I., Yamashita, T., Kojima, T., Kihara, C., Tanaka, T., Imai, K., Nakamura, Y., and Tokino, T. (2002). The *p53* Family Member Genes Are Involved in the Notch Signal Pathway. J. Biol. Chem. *277*, 719–724.
Sauer, M., Bretz, A.C., Beinoraviciute-Kellner, R., Beitzinger, M., Burek, C., Rosenwald, A., Harms, G.S., and Stiewe, T. (2008). C-terminal diversity within the p53 family accounts for differences in DNA binding and transcriptional activity. Nucleic Acids Res. *36*, 1900–1912.
Schade, A.E., Fischer, M., and DeCaprio, J.A. (2019). RB, p130 and p107 differentially repress G1/S and G2/M genes after p53 activation. Nucleic Acids Res. *47*, 11197–11208.
Sen, G.L., Boxer, L.D., Webster, D.E., Bussat, R.T., Qu, K., Zarnegar, B.J., Johnston, D., Siprashvili, Z., and Khavari, P.A. (2012). ZNF750 Is a p63 Target Gene that Induces KLF4 to Drive Terminal Epidermal Differentiation. Dev. Cell *22*, 669–677.
Senoo, M., Pinto, F., Crum, C.P., and McKeon, F. (2007). p63 Is Essential for the Proliferative Potential of Stem Cells in Stratified Epithelia. Cell *129*, 523–536.

Sethi, I., Romano, R.-A., Gluck, C., Smalley, K., Vojtesek, B., Buck, M.J., and Sinha, S. (2015). A global analysis of the complex landscape of isoforms and regulatory networks of p63 in human cells and tissues. BMC Genomics *16*, 584.
Sethi, I., Gluck, C., Zhou, H., Buck, M.J., and Sinha, S. (2017). Evolutionary re-wiring of p63 and the epigenomic regulatory landscape in keratinocytes and its potential implications on species-specific gene expression and phenotypes. Nucleic Acids Res. *45*, 8208–8224.
Somerville, T.D.D., Xu, Y., Miyabayashi, K., Tiriac, H., Cleary, C.R., Maia-Silva, D., Milazzo, J.P., Tuveson, D.A., and Vakoc, C.R. (2018). TP63-Mediated Enhancer Reprogramming Drives the Squamous Subtype of Pancreatic Ductal Adenocarcinoma. Cell Rep. *25*, 1741-1755.e7.
Song, L., and Florea, L. (2015). Rcorrector: efficient and accurate error correction for Illumina RNA-seq reads. Gigascience *4*, 48.
Stewart, H.J.S., Horne, G.A., Bastow, S., and Chevassut, T.J.T. (2013). BRD4 associates with p53 in DNMT3A-mutated leukemia cells and is implicated in apoptosis by the bromodomain inhibitor JQ1. Cancer Med. *2*, 826–835.
Subramanian, A., Tamayo, P., Mootha, V.K., Mukherjee, S., Ebert, B.L., Gillette, M.A., Paulovich, A., Pomeroy, S.L., Golub, T.R., Lander, E.S., et al. (2005). Gene set enrichment analysis: A knowledge-based approach for interpreting genome-wide expression profiles. Proc. Natl. Acad. Sci. *102*, 15545–15550.
Thomason, H.A., Zhou, H., Kouwenhoven, E.N., Dotto, G.-P., Restivo, G., Nguyen, B.-C., Little, H., Dixon, M.J., van Bokhoven, H., and Dixon, J. (2010). Cooperation between the transcription factors p63 and IRF6 is essential to prevent cleft palate in mice. J. Clin. Invest. *120*, 1561–1569.
Tichý, V., Navrátilová, L., Adámik, M., Fojta, M., and Brázdová, M. (2013). Redox state of p63 and p73 core domains regulates sequence-specific DNA binding. Biochem. Biophys. Res. Commun. *433*, 445–449.
Truong, A.B., Kretz, M., Ridky, T.W., Kimmel, R., and Khavari, P.A. (2006). p63 regulates proliferation and differentiation of developmentally mature keratinocytes. Genes Dev. *20*, 3185–3197.
Usui, A., Hoshino, I., Akutsu, Y., Sakata, H., Nishimori, T., Murakami, K., Kano, M., Shuto, K., and Matsubara, H. (2012). The molecular role of Fra-1 and its prognostic significance in human esophageal squamous cell carcinoma. Cancer *118*, 3387–3396.
Uxa, S., Bernhart, S.H., Mages, C.F.S., Fischer, M., Kohler, R., Hoffmann, S., Stadler, P.F., Engeland, K., and Müller, G.A. (2019). DREAM and RB cooperate to induce gene repression and cell-cycle arrest in response to p53 activation. Nucleic Acids Res. *47*, 9087–9103.
Verfaillie, A., Svetlichnyy, D., Imrichova, H., Davie, K., Fiers, M., Atak, Z.K., Hulselmans, G., Christiaens, V., and Aerts, S. (2016). Multiplex enhancer-reporter assays uncover unsophisticated TP53 enhancer logic. Genome Res. *26*, 882–895.
Vyas, P., Beno, I., Xi, Z., Stein, Y., Golovenko, D., Kessler, N., Rotter, V., Shakked, Z., and Haran, T.E. (2017). Diverse p53/DNA binding modes expand the repertoire of p53 response elements. Proc. Natl. Acad. Sci. U. S. A. *114*, 10624–10629.
Wang, L., Wang, S., and Li, W. (2012). RSeQC: quality control of RNA-seq experiments. Bioinformatics *28*, 2184–2185.
Watanabe, H., Ma, Q., Peng, S., Adelmant, G., Swain, D., Song, W., Fox, C., Francis, J.M., Pedamallu, C.S., DeLuca, D.S., et al. (2014). SOX2 and p63 colocalize at genetic loci in squamous cell carcinomas. J. Clin. Invest. *124*, 1636–1645.
Westfall, M.D., Mays, D.J., Sniezek, J.C., and Pietenpol, J.A. (2003). The Np63 Phosphoprotein Binds the p21 and 14-3-3 Promoters In Vivo and Has Transcriptional Repressor Activity That Is Reduced by Hay-Wells Syndrome-Derived Mutations. Mol. Cell. Biol. *23*, 2264–2276.
Whitfield, M.L., George, L.K., Grant, G.D., and Perou, C.M. (2006). Common markers of proliferation. Nat. Rev. Cancer *6*, 99–106.
Wu, N., Rollin, J., Masse, I., Lamartine, J., and Gidrol, X. (2012). p63 regulates human keratinocyte proliferation via MYC-regulated gene network and differentiation commitment through cell adhesion-related gene network. J. Biol. Chem. *287*, 5627–5638.
Yan, W., and Chen, X. (2006). GPX2, a Direct Target of p63, Inhibits Oxidative Stress-

induced Apoptosis in a p53-dependent Manner. J. Biol. Chem. *281*, 7856–7862.
Yang, A., Kaghad, M., Wang, Y., Gillett, E., Fleming, M.D., Dötsch, V., Andrews, N.C., Caput, D., and McKeon, F. (1998). P63, a P53 Homolog At 3Q27–29, Encodes Multiple Products With Transactivating, Death-Inducing, and Dominant-Negative Activities. Mol. Cell *2*, 305–316.
Yang, A., Schweitzer, R., Sun, D., Kaghad, M., Walker, N., Bronson, R.T., Tabin, C., Sharpe, A., Caput, D., Crum, C., et al. (1999). p63 is essential for regenerative proliferation in limb, craniofacial and epithelial development. Nature *398*, 714–718.
Yang, A., Zhu, Z., Kapranov, P., McKeon, F., Church, G.M., R, T., Gingeras, T.R., and Struhl, K. (2006). Relationships between p63 Binding, DNA Sequence, Transcription Activity, and Biological Function in Human Cells. Mol. Cell *24*, 593–602.
Zarnegar, B.J., Webster, D.E., Lopez-Pajares, V., Vander Stoep Hunt, B., Qu, K., Yan, K.J., Berk, D.R., Sen, G.L., and Khavari, P.A. (2012). Genomic profiling of a human organotypic model of AEC syndrome reveals ZNF750 as an essential downstream target of mutant TP63. Am. J. Hum. Genet. *91*, 435–443.
Zhang, Q., Huang, D., Zhang, Z., Feng, Y., Fu, M., Wei, M., Zhou, J., Huang, Y., Liu, S., and Shi, R. (2019). High expression of TMEM40 contributes to progressive features of tongue squamous cell carcinoma. Oncol. Rep. *41*, 154–164.
Zheng, L., Zhao, Z., Rong, L., Xue, L., and Song, Y. (2019a). RASSF6-TRIM16 axis promotes cell proliferation, migration and invasion in esophageal squamous cell carcinoma. J. Genet. Genomics.
Zheng, R., Wan, C., Mei, S., Qin, Q., Wu, Q., Sun, H., Chen, C.-H., Brown, M., Zhang, X., Meyer, C.A., et al. (2019b). Cistrome Data Browser: expanded datasets and new tools for gene regulatory analysis. Nucleic Acids Res. *47*, D729–D735.

Figure 1

Meta-analysis of p63-dependent gene regulation. (A) Distribution of the number of genes found in each of the *p63 Expression Score* groups. Because *p63 Expression Score* group '13' and '-12' contained only 2 genes they were included in group '12' and '-11', respectively, for further analyses. **(B)** 16 datasets on p63-dependent gene expression from 11 studies. EE – exogenous p63 expression; sh KD – shRNA-mediated knockdown; si KD – siRNA-mediated knockdown; KO - sgRNA-mediated knockout **(C)** A heatmap displaying the regulation of 15 genes with positive and 15 genes with negative *p63 Expression Scores*. *GAPDH* and *GAPDHS* represent negative controls.

Figure 2

Gene sets enriched among genes commonly regulated by p63. Enrichment of **(A, B, C, E)** MSigDB gene sets or **(D)** genes up- and down-regulated across squamous cell cancers (SCC) (Campbell et al., 2018) among genes ranked by the *p63 Expression Score*.

Figure 3

Transcription factors in the p63 GRN. (A) Significant (adj.p-value ≤ 0.05) enrichment of TF binding at genes with a *p63 Expression Score* ≥ 8 (green) or ≤ -8 (red) as identified by Enrichr (Kuleshov et al., 2016). **(B)** Enrichment of MSigDB gene sets among genes ranked by the *p63 Expression Score* **(C)** The violin blot displays the $\log_2$(fold-change) of previously

collected high confidence DREAM target genes (Fischer et al., 2016a) across the 16 p63-dependent gene expression profiling datasets.

Figure 4

p63 and p53 regulate largely distinct target gene sets. (A) The *p63 Expression Score* compared to the previously published *p53 Expression Score* that was generated using the same meta-analysis approach (Fischer et al., 2016a) for all 16,198 genes for which both scores were available. **(B)** The violin blot displays the $\log_2$(fold-change) of previously collected high confidence direct p53 target genes (Fischer, 2017) across the 16 p63-dependent gene expression profiling datasets. The data indicates a large degree of independence of p53 targets from p63-dependent expression.

Figure 5

The p63 and p53 DNA binding landscape. (A and B) The number of p63 and p53 binding peaks sorted by the number of datasets that commonly identified/support the peak. **(C)** The number of p53 and p63 peaks identified in the 28 p53 and 20 p63 ChIP-seq datasets, respectively. **(D)** The relative number of 'known' p53 and p63 motifs found by HOMER v4.10 (Heinz et al., 2010) under p53 and p63 peaks, respectively, with increasing dataset support. **(E)** Schematic of 'p53', 'p63' and 'p53+p63' peak selection for further analyses. **(F)** *De novo* motif search results from HOMER v4.10 (Heinz et al., 2010) for the 'p53+p63', 'p53', and 'p63' peak sets. The first round of motif search identified the 'primary' motif in each peak set. Using an iterative approach, all peaks that contained the 'primary' motif were removed and the *de novo* motif search was repeated. This iterative approach was followed until no more p53/p63-like motif was identified.

Figure 6

The DNA binding landscape of p53. DNA sites occupied by p53 in at least 5 datasets were searched iterative with the motifs identified by our iterative *de novo* search (Figure 5F). We searched first for the primary 'p53+p63' motif and among all remaining sites for the primary 'p53' motif. All other 'p53+p63' and 'p53' motifs were searched subsequently.

Figure 7

The DNA binding landscape of p63. DNA sites occupied by p63 in at least 5 datasets were searched iterative with the motifs identified by our iterative *de novo* search (Figure 5F). We searched first for the primary 'p53+p63' motif and among all remaining sites for the primary 'p63' motif. All other 'p53+p63' and 'p63' motifs were searched subsequently (Supplementary Table S3).

Figure 8

High-probability direct p63 target genes. Genes identified as significantly up- or down-regulated in at least the half of all datasets (|*p63 Expression Score*| ≥ 8) that are linked to p63 binding sites supported by at least half of all datasets (≥ 10) through binding within 5 kb from their TSS or through double-elite enhancer:gene associations (Fishilevich et al., 2017). Using these thresholds we identified 138 and 42 high-probability candidates as directly up- and down-regulated by p63, respectively. Gene names marked in red are also up- or down-regulated across SCCs (Campbell et al., 2018).

Figure 9

p63/SCC 28-gene signature correlates with poorer survival in HNSC. Kaplan-Meier plots of TCGA HNSC patient survival data. **(A**) Patients were subdivided in four equally sized subgroups based on expression levels of the 28-gene signature. The results suggest a poorer survival of patients with an up-regulated expression of the signature genes. **(B)** To corroborate this finding patients of the subgroups low-med, med-high, and high from (A) were joined to form a new high group.

Supplementary Figure 1

(A and B) Correlation between dataset support for p53 and p63 binding. (C to F) Correlation between HOMER motif score for primary and secondary 'p53+p63' motifs and dataset support for **(C and D)** p53 binding or **(E and F)** p63 binding.

Supplementary Figure 2

Correlation between HOMER motif score for primary, secondary and tertiary **(A to C)** 'p53' motifs or **(D to F)** 'p63' motifs and dataset support for **(A to C)** p53 binding or **(D to F)** p63 binding.

Supplementary Figure 3

Top motifs co-enriched with primary 'p53+p63', 'p53', and 'p63' motifs at the respective DNA sites.

Supplementary Figure 4

Top 20 TFs with ChIP-seq peak sets similar to **(A)** the common p53+p63 sites, **(B)** the unique p53 sites, and **(C)** the unique p63 sites (Figure 5E) as identified using CistromeDB toolkit. Of note, some TP53 ChIP-seq datasets are wrongly labeled "T" in the database.

Riege *et al.*, Figure 1

A

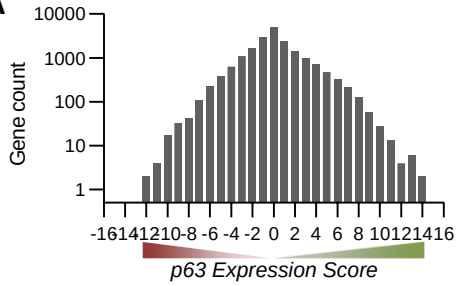

B

Ref	p63 status	cells	platform	# genes covered	# genes sig. regulated up	# genes sig. regulated down
33	EE	MCF10A	microarray	11,358	1,291	1,716
	sh KD	MCF10A		11,358	1,893	2,047
34	EE	KC	microarray	17,883	4,119	4,119
	si KD	KC		17,883	1,951	3,396
36	si KD	HaCaT	microarray	11,580	1,046	873
37	sh KD	H226	microarray	16,470	2,264	1,890
38	sh KD	KYSE70	RNA-seq	12,866	354	580
39	sh KD	KC	RNA-seq	17,219	4,475	4,620
40	sh KD	HaCaT	microarray	16,403	4,386	2,618
	sh KD	FaDu		16,403	1,512	1,057
41	sh KD	H226	RNA-seq	15,984	4,053	4,550
42	sh KD / KO	BxPC3	RNA-seq	16,153	871	1,373
	EE	SUIT2		12,756	1,317	927
43	sh KD	MCF10A	RNA-seq	12,968	2,105	1,568
	sh KD +Nutlin	MCF10A		13,180	2,940	2,198
35	EE	BJ	RNA-seq	16,464	2,530	1,544

C

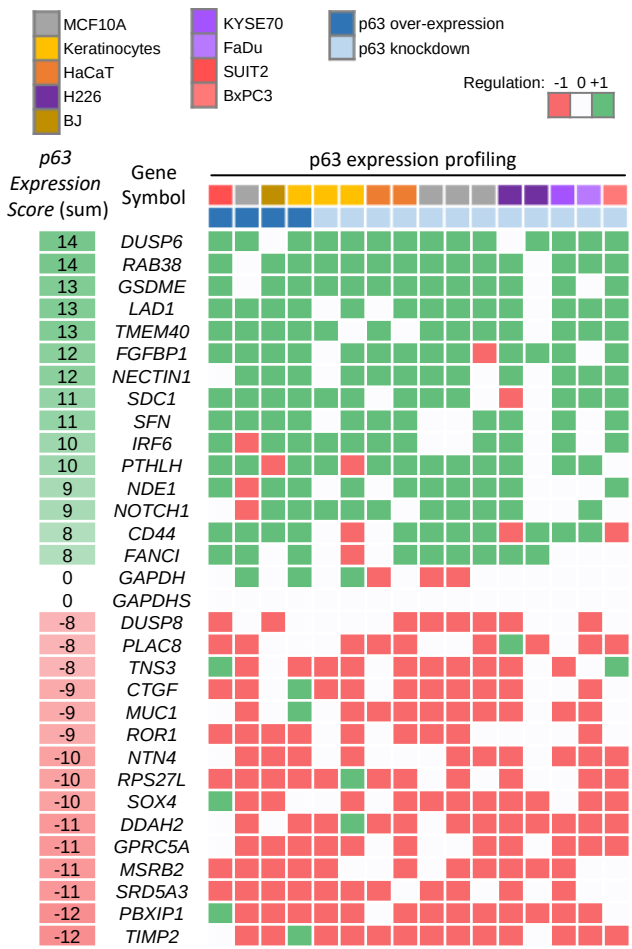

Riege *et al*., Figure 2

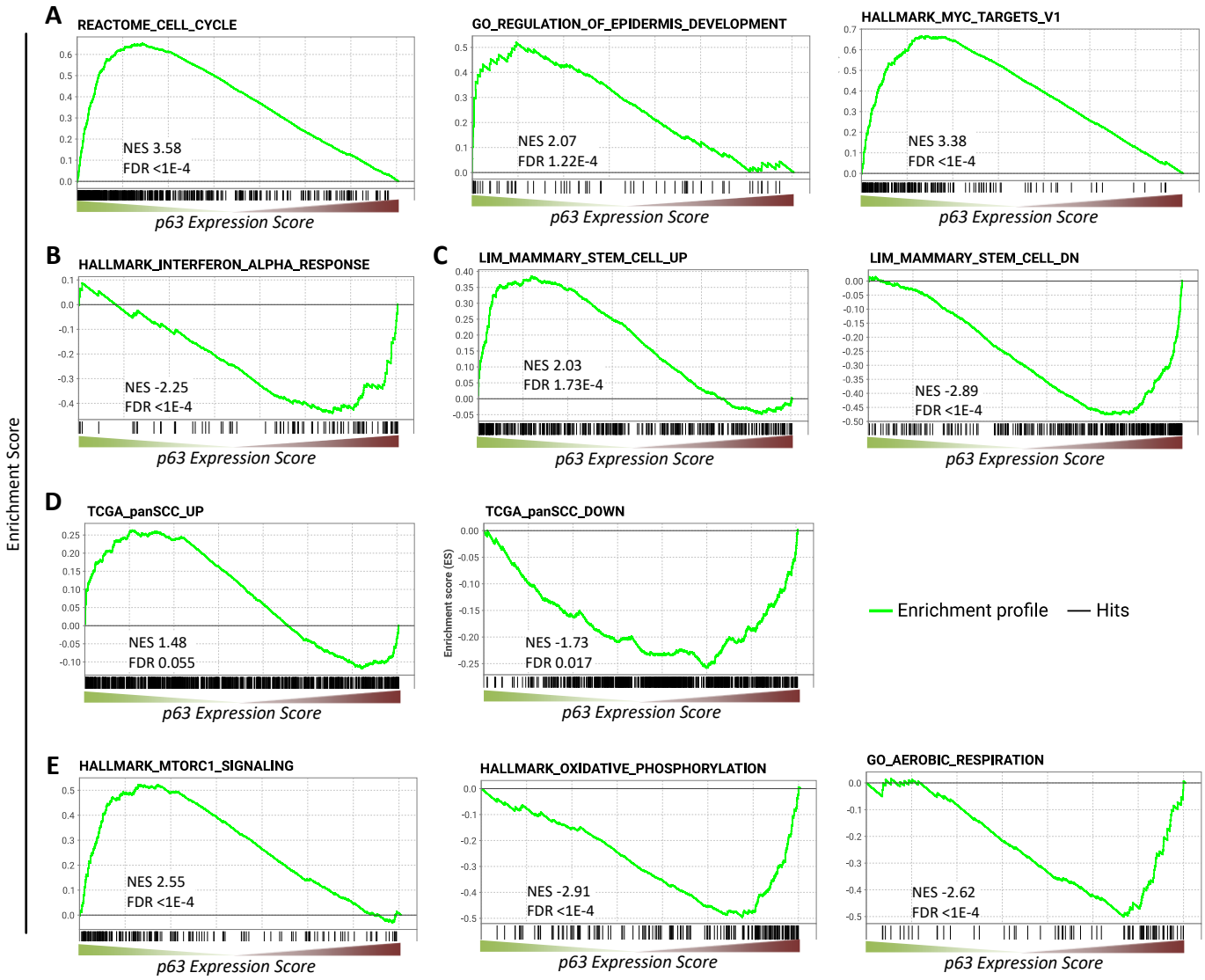

Riege *et al*., Figure 3

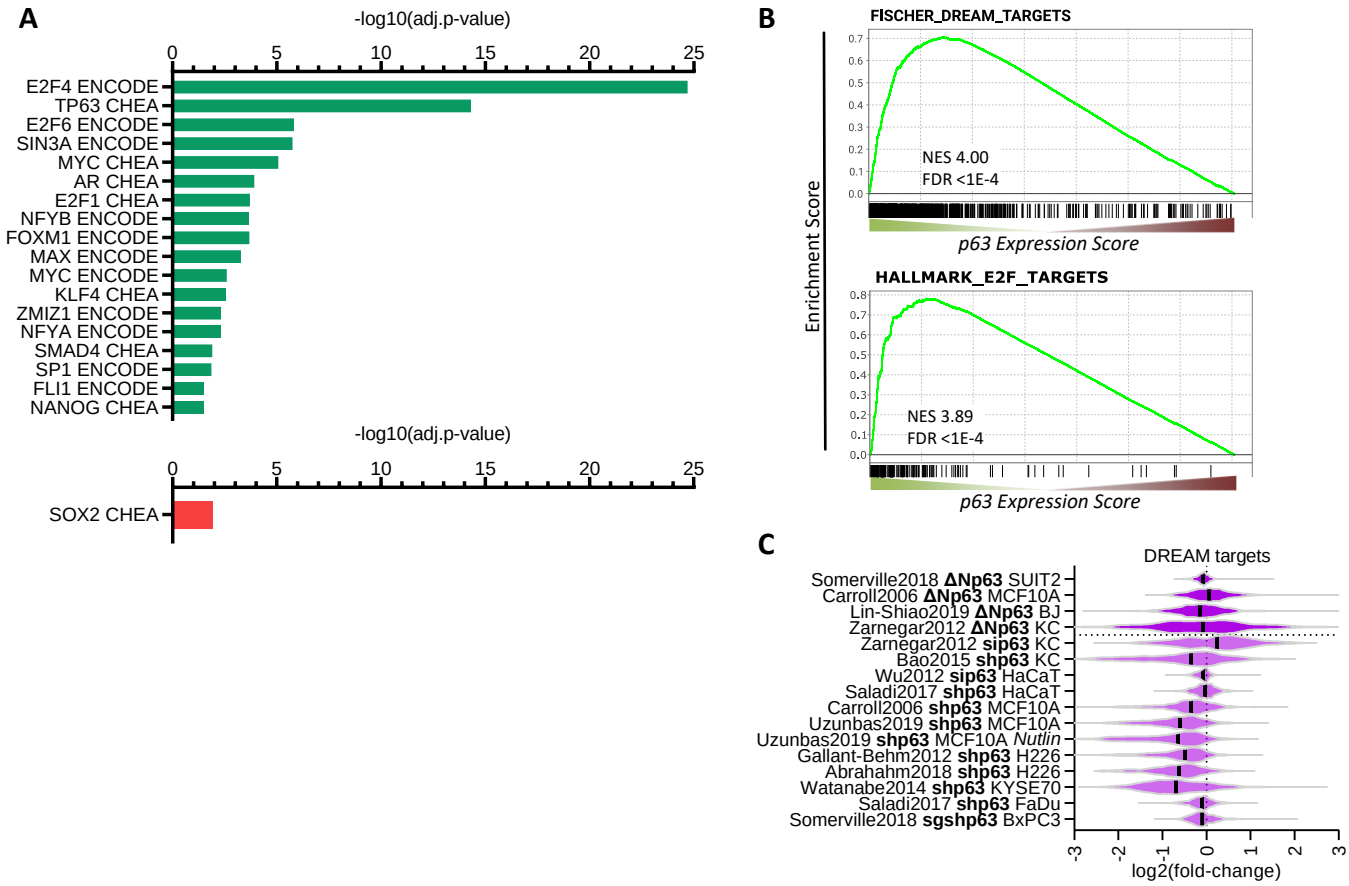

Riege *et al*., Figure 4

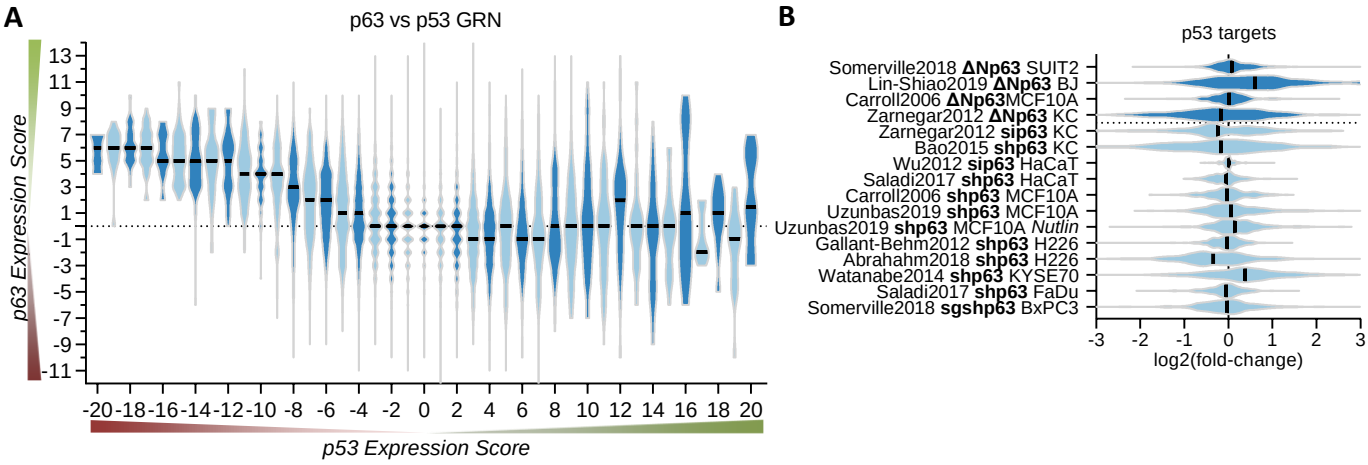

Riege *et al.*, Figure 5

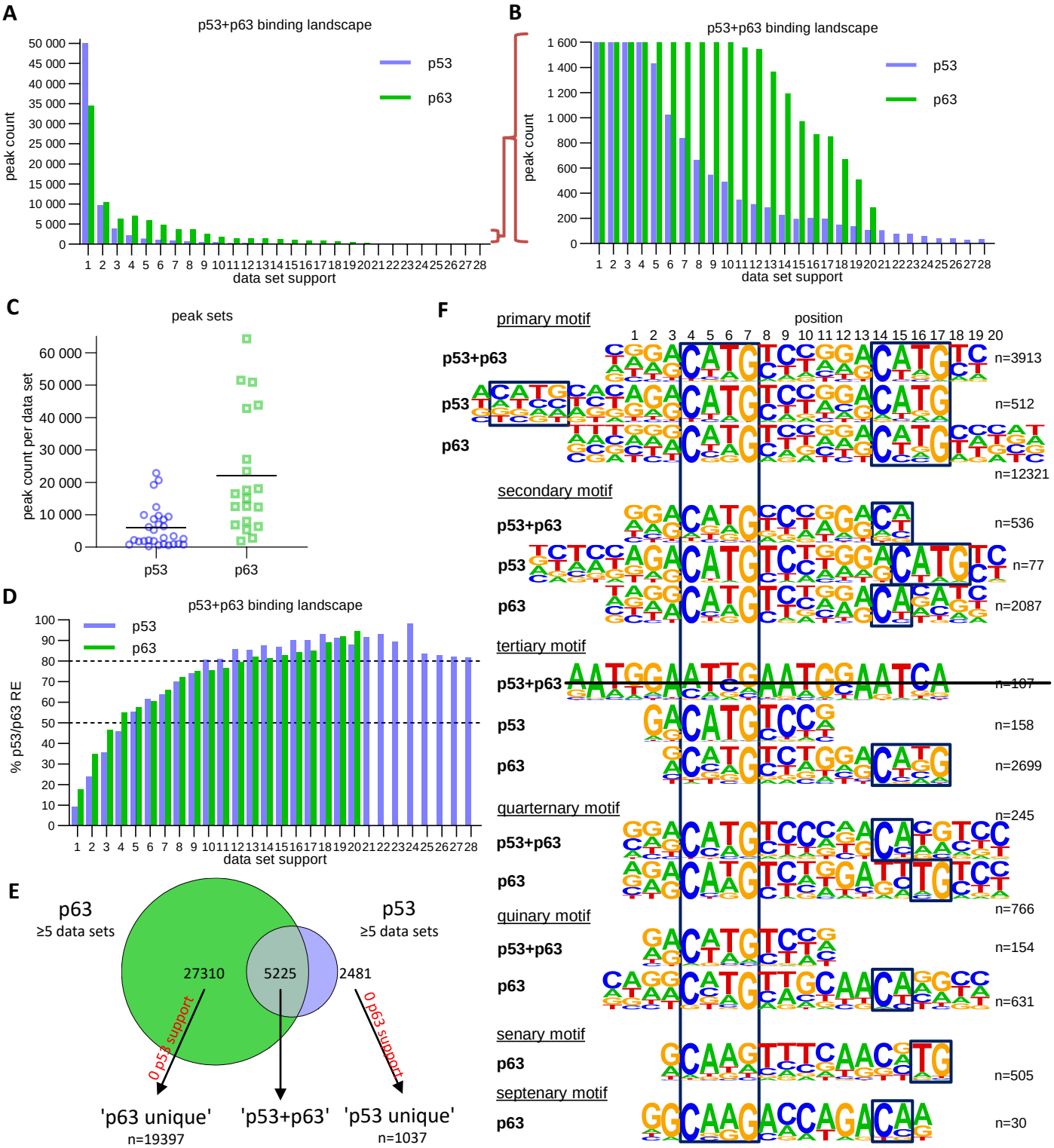

Riege *et al*., Figure 6

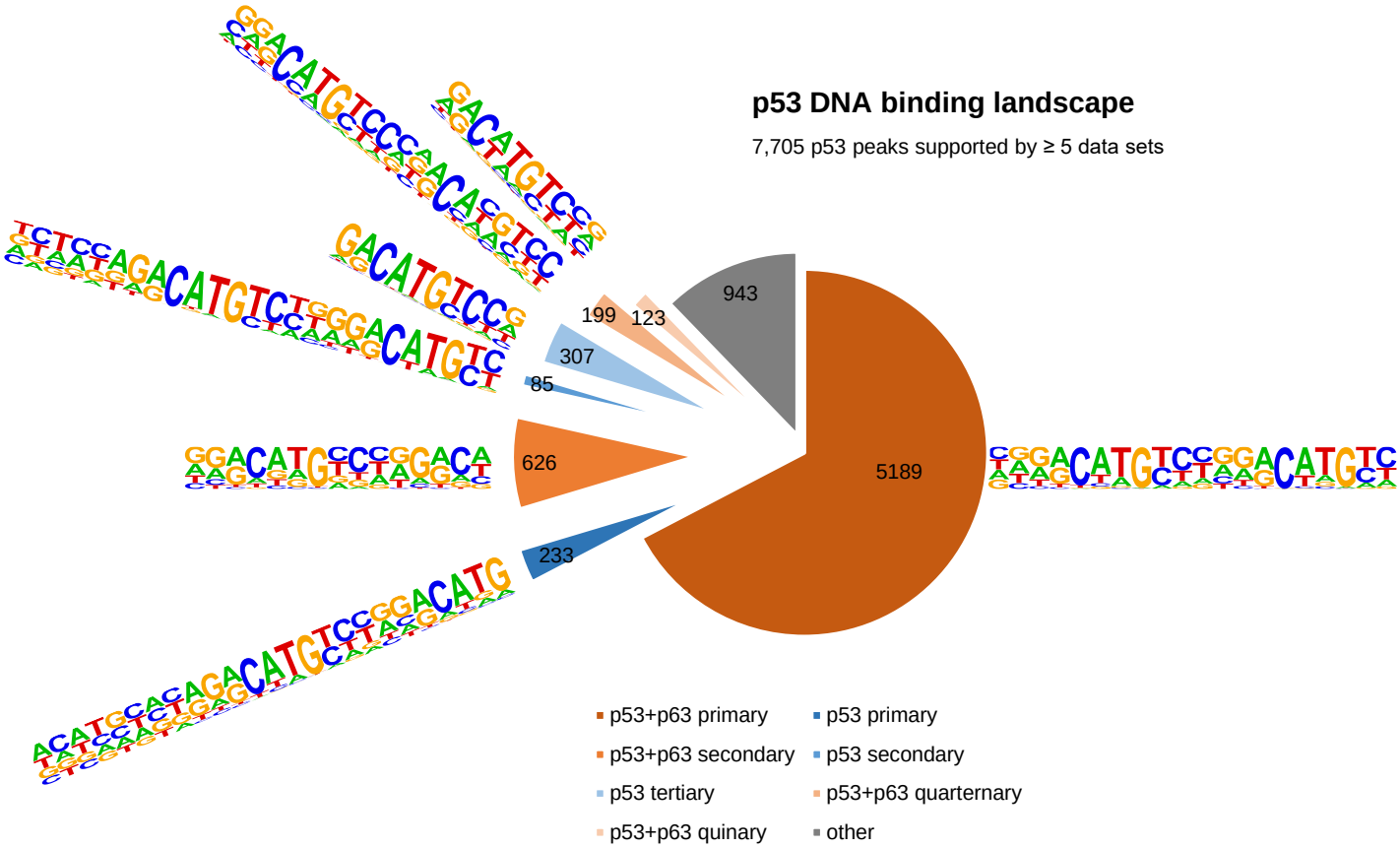

Riege *et al*., Figure 7

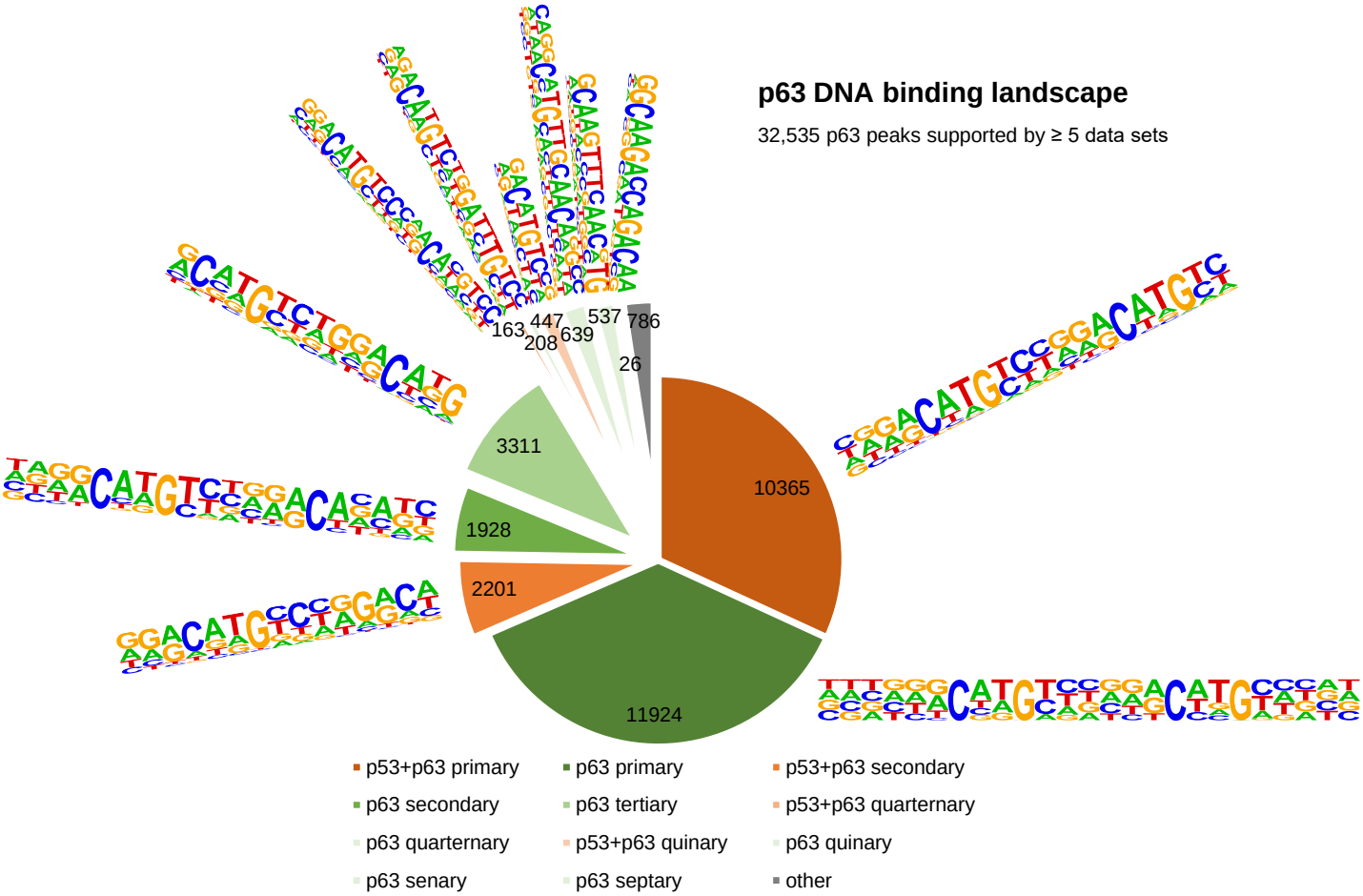

Riege *et al.*, Figure 8
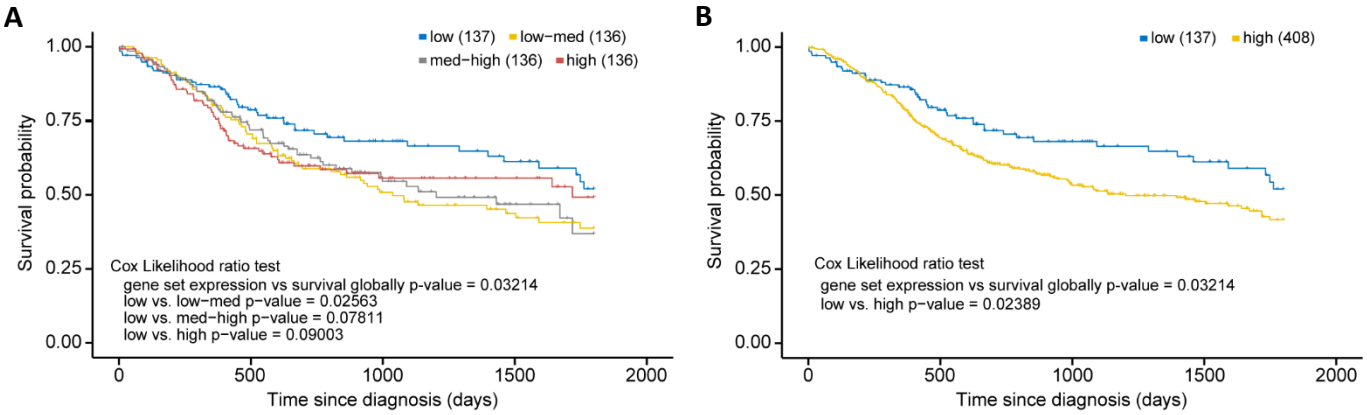
Riege *et al*., Figure 9